pH Sensing Characteristics of Extended-Gate Field-Effect Transistor Based on Al-Doped ZnO Nanostructures Hydrothermally Synthesized at Low Temperatures

Po-Yu Yang, Jyh-Liang Wang, Po-Chun Chiu, Jung-Chuan Chou, Cheng-Wei Chen, Hung-Hsien Li, and Huang-Chung Cheng

***Abstract*—The pH sensing properties of an extended-gate field-effect transistor (EGFET) with Al-doped ZnO (AZO) nanostructures are investigated. The AZO nanostructures with different Al dosages were synthesized on AZO/glass substrate via a simple hydrothermal growth method at 85 °C. The pH sensing characteristics of pH-EGFET sensors with an Al dosage of 1.98 at% can exhibit a higher voltage sensitivity of 57.95 mV/pH, a larger linearity of 0.9998, and a wide sensing range of pH 1–13, attributed to the well-aligned nanowire (NW) array, superior crystallinity, less structural defects, and better conductivity. Consequently, the hydrothermally grown AZO NWs demonstrate superior pH sensing characteristics and reveal the potentials for flexible and disposable biosensors.**

***Index Terms*—Al-doped zinc oxide (AZO), extended-gate field-effect transistor (EGFET), hydrothermal method, low temperature.**

I. Introduction

EXTENDED-GATE field-effect transistor (EGFET) was investigated by Spiegel *et al.* in 1983 [1]. The EGFET has more advantages than the conventional ion-sensitive field-effect transistor (ISFET) [2], such as low cost, simpler to passivate and package, high shape flexibility of the extended-gate structure, less insensitivity induced by temperature and light fluctuations, and better long-term stability [3]. The surface ion adsorption mechanisms of pH-sensitive membranes in ISFET and EGFET are the same. The principal distinction between pH-ISFET and pH-EGFET sensors is the impedance of sensing films [4]. The insulating membranes (i.e., SiO_2, Al_2O_3, and Si_3N_4) are commonly used in ISFET and present a very low sensitivity when applied in EGFET. The sensing gate of EGFET must be a high-conductivity electrode that can transmit sensing signals easily [5]. Recently, 1-D ZnO nanostructures have attracted considerable attention as the pH-sensitive membranes, owing to the high surface-to-volume ratio, thermal stability, chemical stability, electrochemical activity, electron communication features, mechanical strength, and nontoxicity [6]. Nevertheless, intrinsic ZnO exhibits high resistivity and low conductivity. The ZnO doped with group III metal elements (i.e., Al, In, and Ga) could enhance the conductivities [7]. Al-doped ZnO (AZO) nanowires (NWs) and nanotubes have been presented for high conductance and crystal quality [8], suggesting lower resistivity and higher carrier mobility. However, to date, the low-temperature fabrications of AZO nanostructure arrays are not well investigated, and their according pH-sensitive properties have not been reported yet. In this letter, the physical and pH sensing characteristics of the low-temperature hydrothermally grown undoped ZnO and AZO nanostructures with various Al dosages are systematically addressed.

Manuscript received July 4, 2011; revised July 26, 2011; accepted August 2, 2011. Date of publication September 14, 2011; date of current version October 26, 2011. This work was supported by the National Science Council of Taiwan under Contract NSC 99-2221-E-009-168-MY3. The review of this letter was arranged by Editor W. S. Wong.

P.-Y. Yang, P.-C. Chiu, H.-H. Li, and H.-C. Cheng are with the Department of Electronics Engineering and the Institute of Electronics, National Chiao Tung University, Hsinchu 300, Taiwan (e-mail: youngboy.ee96g@g2.nctu.edu.tw).

J.-L. Wang is with the Department of Electronics Engineering, Ming Chi University of Technology, Taipei 243, Taiwan.

J.-C. Chou and C.-W. Chen are with the Graduate School of Engineering Science and Technology, National Yunlin University of Science and Technology, Yunlin 640, Taiwan.

Color versions of one or more of the figures in this letter are available online at http://ieeexplore.ieee.org.

Digital Object Identifier 10.1109/LED.2011.2164230

II. Device Structure and Fabrication

In our earlier study [9], the AZO nanostructures with various Al dosages were synthesized successfully on AZO/glass substrate by a hydrothermal growth method at 85 °C. After the hydrothermal growth, the samples were bound to metal wire with silver paste, packaged with epoxy resin, and then baked in an oven for 30 min at 120 °C to form sensing heads. Epoxy resin was used to avoid the leakage current and define the sensing window as 2×2 mm^2. Subsequently, a Keithley 236 semiconductor parameter analyzer was used to measure the current–voltage (I–V) characteristics of the pH-EGFET sensor in different phosphate buffer solutions (PBSs). The morphologies of the grown undoped ZnO and AZO nanostructures were observed by field-emission scanning electron microscopy (FE-SEM, Hitachi S-4700I). The crystallinity of samples was investigated using high-resolution transmission electron microscopy (HRTEM, JEOL JEM-3000F). The optical emission properties of undoped ZnO and AZO nanostructures were examined by photoluminescence (PL) spectra with He–Cd laser (i.e., $\lambda =$ 325 nm) excitation. The experimental compositions of Al in the AZO nanostructures were checked by X-ray photoelectron spectroscopy (Physical Electronics PHI-1600) as 0 at%, 1.98 at%, 3.35 at%, and 6.27 at%, corresponding to the controlled Al dosages of 0 at%, 3 at%, 5 at%, and 7 at%.

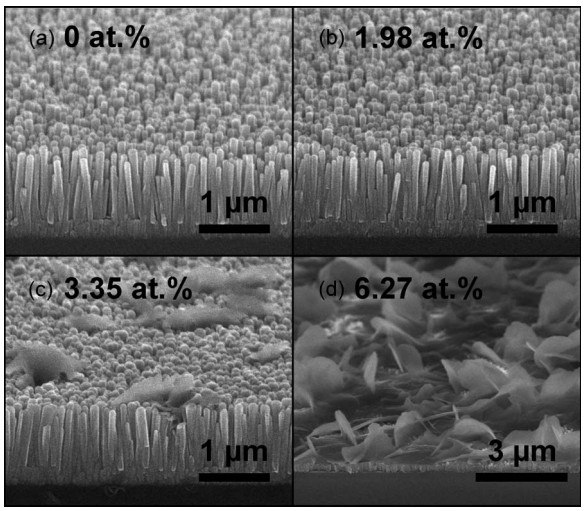

Fig. 1. FE-SEM 45°-tilt-view images of AZO nanostructures grown on the AZO/glass substrate with different Al dosages of (a) 0 at% (undoped ZnO), (b) 1.98 at%, (c) 3.35 at%, and (d) 6.27 at%.

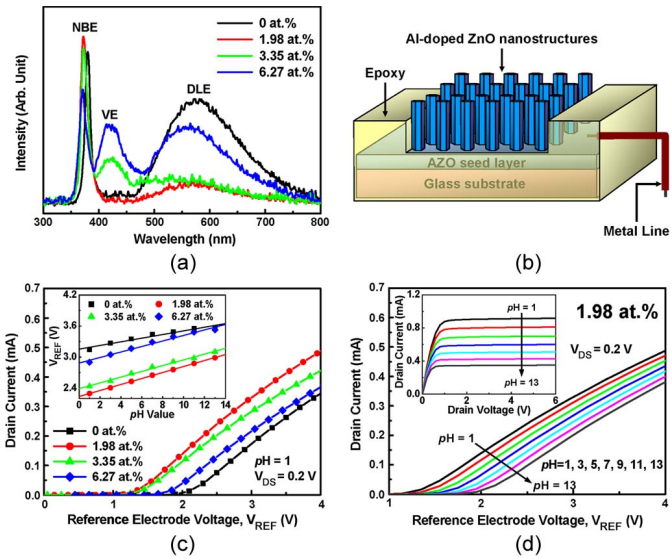

Fig. 2. (a) Room-temperature PL emission spectra of undoped ZnO and AZO nanostructures. (b) Schematic diagram of the sensing head structure. (c) $I_{\rm DS}$–$V_{\rm REF}$ curves for the pH-EGFET sensors with various Al dosages at pH 1. The inset gives the sensitivity curves that the reference electrode potential varied as a function of pH value with fixed $I_{\rm DS} = 0.2$ mA and $V_{\rm DS} = 0.2$ V. (d) $I_{\rm DS}$–$V_{\rm REF}$ curve of 1.98 at% AZO pH-EGFET immersed in PBS at pH 1–13 for the linear regime of MOSFET operation. The inset also shows its pH response in the saturation regime of MOSFET operation with $V_{\rm REF} = 3$ V.

III. Results and Discussion

The FE-SEM images of undoped ZnO and AZO nanostructures grown on the AZO/glass substrate are shown in Fig. 1. While the Al dosage was less than 1.98 at%, only NWs are observed. Both the undoped and lightly Al-doped ZnO NWs are well ordered and vertically aligned with similarly specific dimensions (i.e., an average length of $\sim$1 μm and a diameter of $\sim$100 nm). Contrarily, nanosheets (NSs) are obtained while Al dosages are above 1.98 at%. NWs and NSs coexisted when the Al dosage was 3.35 at%. The sample doped with 6.27 at% Al dosage discloses the remarkable changes on morphology, resulting in complete NSs. Moreover, the HRTEM images (not shown here) exhibit that the lightly Al-doped ($\leqq$ 1.98 at%) NWs are single-crystalline wurtzite structured, and heavily Al-doped (6.27 at%) NSs reveal the polycrystalline ZnO wurtzite crystals [9]. Fig. 2(a) shows the PL spectra of undoped ZnO and AZO nanostructures. The PL spectra can be classified as three components: One is UV emission, owing to the near band-edge emission (NBE) [10], another is the deep level emission (DLE) in the visible region due to the presence of structural defects (i.e., oxygen vacancies, oxygen interstitials, zinc vacancies, and zinc interstitials) [11], and the other is violet emission (VE) located at about 420 nm. The less structural defects can exist in the AZO NWs with appropriate Al dosage (i.e., 1.98 at%). The reduced structural defects presumably result from that the Al ions competing with Zn ions to consume the residual O ions and decrease the concentration of oxygen interstitials in the AZO NWs [12]. Contrastively, the intensities of VE and DLE were magnified with the declined intensity of NBE while the Al dosage was increased above 1.98 at%. The violet luminescence was probably related to the radiative defects (i.e., the interface traps existing at grain boundaries) and emitted from the radiative transition between this energy level and the valence band [13]. The higher intensity of violet luminescence can be associated with more grain boundary defects, indicating that the smaller grain sizes and higher density of grain boundaries are obtained in heavily Al-doped ($>$ 1.98 at%) samples. In addition, the NBE emission peak was shifted from 380 to 371 nm as the Al dosage was increased [11], described as blueshift and connected to the Burstein–Moss effect. Fig. 2(b) shows the schematic diagram of a sensing head structure. The flatband voltage increases with the increase of carrier concentration in sensing film [14], resulting in a decrease of pH-EGFET threshold voltage as the Al dosage increases [Fig. 2(c)]. The I–V relationship varied with pH values and can be expressed by using the basic MOSFET expression [14]. The pH sensitivity values were extracted as 35.23, 57.95, 55.61, and 53.34 mV/pH with respect to the Al dosages of 0 at%, 1.98 at%, 3.35 at%, and 6.27 at% in the range of pH 1–13, accordingly. The inset of Fig. 2(c) shows that the linearity values are about 0.9757, 0.9998, 0.9962, and 0.9902, correspondingly. Fig. 2(d) and its inset reveal the saturation and linear regime of $I_{\rm DS}$–$V_{\rm REF}$ curves, respectively, while the 1.98 at% AZO pH-EGFET is immersed in different PBSs. AZO pH-EGFETs with 1.98 at% Al dosage demonstrate the excellent sensitivity (i.e., 57.95 mV/pH) and linearity (i.e., 0.9998) to pH values. A model of energy-band diagrams is proposed to explain the electrical observations. The Fermi level is typically higher than the redox potential of the electrolyte for an n-type semiconductor electrode at open circuit [Fig. 3(a)] [15]. After the contact of ZnO nanostructure electrode and PBS, electrons will therefore be transferred from the electrode into the solution. There is a positive charge associated with the space charge region, bringing upward bending of the band edges by built-in potential $(V_{\rm built-in})$ [Fig. 3(b)]. Furthermore, Fig. 3(c) shows the band-edge bending response to the redox electrolyte without structural defects. Conversely, the semiconductors have a significant density of structural defects between the conduction band and the valence band that can exhibit Fermi level pinning when contacting a liquid electrolyte solution [Fig. 3(d)] [16]. The density and energy distribution of structural defects affect the energy level, work function, and band-bending grade (barrier height) of a semiconductor [17]. When the Al dosage

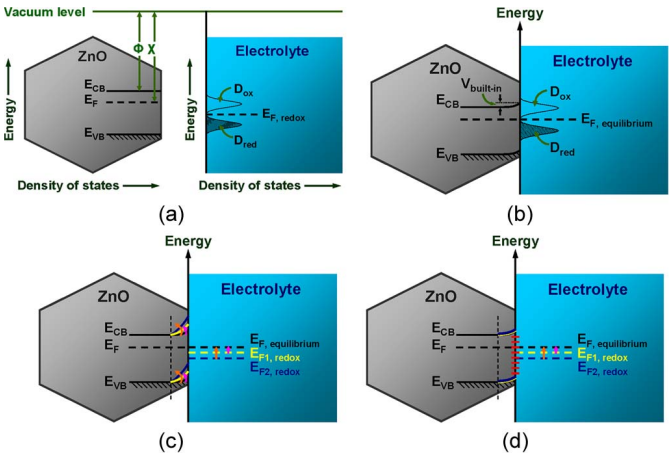

Fig. 3. Energy-band diagrams (a) before and (b) after the contact of ZnO nanostructure electrode and PBS for a system of n-ZnO and redox electrolyte junction, where χ, Φ, $D_{\rm ox}$, $D_{\rm red}$, $E_{\rm CB}$, $E_{\rm VB}$, E_F, $E_{F,\rm redox}$, and $E_{F,\rm equilibrium}$ are the semiconductor electron affinity, work function, a Gaussian distribution of oxidized states versus electron energy, a Gaussian distribution of reduced states versus electron energy, conduction band, valence band, Fermi level, Fermi level of the redox system, and Fermi level at equilibrium system, respectively. The energy levels for the system of n-ZnO and redox electrolyte junction at equilibrium (c) without and (d) with structural defects. E_{F1} and E_{F2} are the Fermi levels of the redox system at different electrolyte systems.

was increased above 1.98 at%, the sensitivity values decrease significantly due to the polycrystals and disorders of NSs. Briefly, 1.98 at% AZO pH-EGFET demonstrates the optimum pH sensing characteristics attributed to the well-aligned NW array, superior crystallinity, and less structural defects, which can profit for carrier lifetime and better conductivity due to the increases of carrier concentration [18].

IV. Conclusion

In summary, AZO nanostructures with various Al dosages were synthesized on AZO/glass substrate by a hydrothermal growth method at 85 °C. The morphologies, crystallinity, and pH sensing properties of AZO nanostructures are functions of Al dosage. AZO nanostructures with proper Al dosage (i.e., 1.98 at%) reveal the well-aligned NW array, superior crystallinity, less structural defects, and better conductivity, resulting in superior pH sensing characteristics (i.e., a higher voltage sensitivity of 57.95 mV/pH, a larger linearity of 0.9998, and a wide sensing range of pH 1–13). A low-temperature hydrothermal growth method has been employed to synthesize the well-aligned arrays of AZO NWs with superior pH sensing characteristics, implying the potential applications in flexible and disposable biosensors.

References

[1] J. Van Der Spiegel, I. Lauks, P. Chan, and D. Babic, "The extended gate chemical sensitive field effect transistor as multi-species microprobe," *Sens. Actuators*, vol. 4, pp. 291–298, Jan. 1983.

[2] P. Bergveld, "Development of an ion sensitive solid-state device for neurophysiological measurement," *IEEE Trans. Biomed. Eng.*, vol. BME-17, no. 1, pp. 70–71, Jan. 1970.

[3] N. H. Chou, J. C. Chou, T. P. Sun, and S. K. Hsiung, "Differential type solid-state urea biosensors based on ion-selective electrodes," *Sens. Actuators B, Chem.*, vol. 130, no. 1, pp. 359–366, Mar. 2008.

[4] J. L. Chiang, J. C. Chou, and Y. C. Chen, "Study of the pH-ISFET and EnFET for biosensor applications," *J. Med. Biol. Eng.*, vol. 21, no. 3, pp. 135–146, Jul. 2001.

[5] J. C. Chou and C. W. Chen, "Fabrication and application of ruthenium-doped titanium dioxide films as electrode material for ion-sensitive extended-gate FETs," *IEEE Sens. J.*, vol. 9, no. 3, pp. 277–284, Mar. 2009.

[6] A. Fulati, S. M. Usman Ali, M. Riaz, G. Amin, O. Nur, and M. Willander, "Miniaturized pH sensors based on zinc oxide nanotubes/nanorods," *Sensors*, vol. 9, no. 11, pp. 8911–8923, Nov. 2009.

[7] J. Zhong, S. Muthukumar, Y. Chen, Y. Lu, H. M. Ng, W. Jiang, and E. L. Garfunkel, "Ga-doped ZnO single-crystal nanotips grown on fused silica by metalorganic chemical vapor deposition," *Appl. Phys. Lett.*, vol. 83, no. 16, pp. 3401–3403, Oct. 2003.

[8] J. Chen, W. Lei, W. Chai, Z. Zhang, C. Li, and X. Zhang, "High field emission enhancement of ZnO-nanorods via hydrothermal synthesis," *Solid State Electron.*, vol. 52, no. 4, pp. 294–298, Feb. 2008.

[9] P. Y. Yang, J. L. Wang, W. C. Tsai, S. J. Wang, J. C. Lin, I. C. Lee, C. T. Chang, and H. C. Cheng, "Field-emission characteristics of Al-doped ZnO nanostructures hydrothermally synthesized at low temperature," *J. Nanosci. Nanotechnol.*, vol. 11, no. 7, pp. 6013–6019, Jul. 2011.

[10] Y. C. Kong, D. P. Yu, B. Zhang, W. Fang, and S. Q. Feng, "Ultraviolet-emitting ZnO nanowires synthesized by a physical vapor deposition approach," *Appl. Phys. Lett.*, vol. 78, no. 4, pp. 407–409, Jan. 2001.

[11] R. C. Wang, C. P. Liu, J. L. Huang, and S. J. Chen, "Single-crystalline AlZnO nanowires/nanotubes synthesized at low temperature," *Appl. Phys. Lett.*, vol. 88, no. 2, pp. 023 111-1–023 111-3, Jan. 2006.

[12] H. W. Kim, M. A. Kebede, and H. S. Kim, "Structural, Raman, and photoluminescence characteristics of ZnO nanowires coated with Al-doped ZnO shell layers," *Curr. Appl. Phys.*, vol. 10, no. 1, pp. 60–63, Jan. 2010.

[13] B. J. Jin, S. Im, and S. Y. Lee, "Violet and UV luminescence emitted from ZnO thin films grown on sapphire by pulsed laser deposition," *Thin Solid Films*, vol. 366, no. 1/2, pp. 107–110, May 2000.

[14] S. M. Sze, *Physics of Semiconductor Devices*, 2nd ed. New York: Wiley, 1981.

[15] S. Al-Hilli and M. Willander, "The pH response and sensing mechanism of n-Type ZnO/Electrolyte interfaces," *Sensors*, vol. 9, no. 9, pp. 7445–7480, Sep. 2009.

[16] R. L. Van Meirhaeghe, F. Cardon, and W. P. Gomes, "A quantitative expression for partial Fermi level pinning at semiconductor/redox electrolyte interfaces," *J. Electroanal. Chem.*, vol. 188, no. 1/2, pp. 287–291, 1985.

[17] J. L. Chiang, J. F. Hsu, S. F. Lee, L. Y. Lee, and H. Y. Liu, "Ion sensitivity of the flowerlike ZnO nanorods synthesized by the hydrothermal process," *J. Vac. Sci. Technol. B*, vol. 27, no. 3, pp. 1462–1465, May 2009.

[18] X. T. Hao, J. Ma, D. H. Zhang, T. L. Yang, H. L. Ma, Y. G. Yang, C. F. Cheng, and J. Huang, "Thickness dependence of structural, optical and electrical properties of ZnO:Al films prepared on flexible substrates," *Appl. Surf. Sci.*, vol. 183, no. 1/2, pp. 137–142, Nov. 2001.